Mon. Not. R. Astron. Soc. **273,** 475–483 (1995)

The power spectrum of density fluctuations in the Zel'dovich approximation

Peter Schneider and Matthias Bartelmann
Max-Planck-Institut für Astrophysik, Postfach 1523, D-85740 Garching, Germany

Accepted 1994 October 16. Received 1994 September 30; in original form 1994 June 16

ABSTRACT

The Zel'dovich approximation, combined with an initial spectrum, appears to yield a surprisingly good prescription of the large-scale matter distribution for the evolution of structure in the Universe; in particular, it describes the evolution of structure fairly accurately well into the non-linear regime, and is thus superior to the standard Eulerian linear perturbation theory. We calculate the evolution of the power spectrum $P(k, a)$ of the density field in the Zel'dovich approximation, which can be reduced to a single one-dimensional integral. The resulting expression reproduces the result from linear perturbation theory for small values of the cosmic scale factor a. On the other hand, the power spectrum as obtained from the Zel'dovich approximation predicts the generation of power on small scales, mainly as a result of the formation of compact structures and caustics. In fact, it is shown that, for $k \to \infty$, $P(k, a)$ behaves like k^{-3} on scales for which dissipative processes are negligible; this asymptotic behaviour is not an artefact of the Zel'dovich approximation, but is due to the occurrence of pancakes. We evaluate the power spectrum for standard hot dark matter (HDM) and cold dark matter (CDM) spectra; in the latter case, we employ the truncated Zel'dovich approximation which has been shown previously to yield much better agreement with the results from N-body simulations in cases where the primordial power spectrum contains large amounts of power on small scales. We obtain a simple fitting formula for the smoothing scale used in the truncated Zel'dovich approximation.

Key words: cosmology: theory – dark matter – large-scale structure of Universe.

1 INTRODUCTION

The formation of large-scale structure in the Universe is believed to occur via the gravitational instability of primordial density fluctuations, and can be investigated by numerical N-body simulations or similar techniques (see, e.g., Padmanabhan 1993). Since such simulations are very time-consuming, several approximation schemes have been developed which yield useful results in some limiting cases. Linear perturbation theory describes the evolution of the density perturbations in the linear regime, i.e. as long as the relative fluctuations $\delta \equiv \delta\rho/\langle\rho\rangle \ll 1$. Perhaps the most successful approximation has been the Zel'dovich approximation, which can be considered as the first-order term of a Lagrangian perturbation theory, specialized to irrotational flows with the peculiar velocity initially being parallel to the peculiar acceleration (see, e.g., Buchert & Ehlers 1993 and references therein). Its simplicity allows a very fast, high-resolution construction of the density field. When compared with the results obtained from N-body simulations, the Zel'dovich approximation yields surprisingly accurate results, which remain valid far into the non-linear regime (e.g., Melott 1994). Only after the first caustics are formed does the Zel'dovich approximation become inaccurate, in that the compact structures are dissolved again because of the lack of self-gravity in the approximation scheme. It is for this reason that the Zel'dovich approximation is most accurate for high redshifts, and for cosmological theories that involve relatively little power on small scales, such as the HDM model. In contrast, the CDM model contains appreciable power on small scales, such that low-mass objects are predicted to form first; hence caustics will form early, and the Zel'dovich approximation soon becomes inaccurate on small scales (i.e., scales smaller than the current scale of non-linearity). If one is interested predominantly in the structure on large scales, however, the Zel'dovich approximation still provides a useful means for describing some aspects of the large-scale structure. Modifications of the Zel'dovich

approximation, such as the adhesion approximation (see, e.g., Weinberg & Gunn 1990), the truncated Zel'dovich approximation (Coles, Melott & Shandarin 1993; the truncation we use later is slightly different from theirs), or higher-order Zel'dovich approximations (Buchert 1994), provide even more accurate results when compared to the results of *N*-body simulations (Melott, Buchert & Weiss 1994).

Motivated by the success of the Zel'dovich approximation, we have calculated the power spectrum predicted by this theory following, in part, the ideas of Mann, Heavens & Peacock (1993; hereafter MHP). We expect that the non-linear evolution described by the Zel'dovich approximation will yield power on small scales, even if the initial spectrum is effectively devoid of small-scale power, as is the case for an HDM initial spectrum. As we shall show in Section 2, the description of particle trajectories in the Zel'dovich approximation allows us to reduce the equation for the power spectrum to a one-dimensional integral, which is readily integrated. For an HDM model, we find that power is indeed generated on small scales, increasing with decreasing redshifts. For the CDM model, the power on small scales is reduced because of early shell crossings. By introducing a smoothing scale into the initial spectrum (truncated Zel'dovich approximation), however, much of this power is preserved if the smoothing scale is adapted to the redshift where the power spectrum is calculated. We have obtained the smoothing scale by considering the two-point correlation function $\xi(x, a)$, which attains, for fixed (small) separations x, a maximum value as a function of the smoothing scale $R_{\rm sm}$; a simple approximation formula for $R_{\rm sm}$ as a function of the cosmic scale factor a is obtained. Nevertheless, this smoothing procedure does not cure the basic shortcoming of the Zel'dovich approximation, i.e. compact structures decay after their formation. This drawback is most severe for CDM: in this model, the spectrum predicted within the Zel'dovich approximation has less power on small scales than that predicted by linear perturbation theory (cf. Fig. 2 later).

The rest of this paper is organized as follows: in Section 2, we derive the general expressions for the two-point correlation function and the power spectrum in the framework of the Zel'dovich approximation, assuming that the primordial fluctuations can be considered as a Gaussian random field; the power spectra for the HDM and CDM models are presented in Section 3, and a brief summary is given in Section 4. Two appendices contain some technical details of the calculations.

After submission of this paper, we were informed by John Peacock that the basic result of this paper, equation (2.15), has been derived before by Bond & Couchman and was published in a CITA preprint (Bond & Couchman 1987). This result was also quoted, and a brief derivation given, in Taylor (1993). Nevertheless, we hope that the detailed derivation given in Section 2 and, in particular, the explicit form (2.16) of the power spectrum, together with explicit expressions for its numerical evaluation in Appendix B, will be found useful.

2 BASIC EQUATIONS AND DEFINITIONS

The starting point of our consideration is a density-contrast field

$$\delta(\boldsymbol{x}, a)=\frac{\rho(\boldsymbol{x}, a)-\langle\rho\rangle(a)}{\langle\rho\rangle(a)}, \tag{2.1}$$

where $\rho(\boldsymbol{x}, a)$ is the density at comoving position $\boldsymbol{x}$ at a time characterized by the expansion factor $a=1/(1+z)$, with z being the redshift, and $\langle\rho\rangle(a)=\rho_0/a^3$ is the mean density at 'time' a (throughout this paper, we characterize the cosmic time t by the expansion factor); a is normalized such that $a=1$ today. At some early time $a_{\rm i}\ll 1$, we assume that the initial density-contrast field $\delta_{\rm i}$ is a Gaussian random field, and we denote the density contrast, linearly extrapolated to the current epoch, by δ_0:

$$\delta_0(\boldsymbol{q})=\frac{1}{a_{\rm i}}\,\delta_{\rm i}(\boldsymbol{q}). \tag{2.2}$$

We now employ the Zel'dovich (1970) approximation for the evolution of the density contrast (see also Buchert & Ehlers 1993; Melott 1994, and references therein). If $\boldsymbol{q}$ denotes the comoving coordinate of a particle (or a 'fluid' element) on the hypersurface defined by $a=a_{\rm i}$, the Zel'dovich approximation describes its comoving coordinate $\boldsymbol{x}$ at some later time a by

$$\boldsymbol{x}(\boldsymbol{q}, a)=\boldsymbol{q}+b(a)\nabla\Phi_0(\boldsymbol{q}), \tag{2.3}$$

where $b(a)$ is a function whose time dependence is determined by requiring that equation (2.3) yield the correct linear evolution, which leads to a second-order differential equation for b (see Buchert 1992). Its two linearly independent solutions describe growing and decaying modes, respectively. For simplicity, we confine our treatment to the Einstein–de Sitter universe, and consider only the growing mode of the perturbation spectrum; then $b=a-a_{\rm i}\approx a$ for $a\gg a_{\rm i}$. We also restrict our attention to potential flows, since the rotational components of the velocity field quickly decay with increasing scale factor. The potential $\Phi_0(\boldsymbol{q})$ in equation (2.3) is related to the density contrast via the 'Poisson equation'

$$\nabla^2\Phi_0(\boldsymbol{q})=-\,\delta_0(\boldsymbol{q}). \tag{2.4}$$

Note that equation (2.4) does not specify the potential Φ_0 uniquely, since any solution of Laplace's equation can be added. If we specify Φ_0 to be a homogeneous, isotropic Gaussian random field, however, then (i) Φ_0 is uniquely determined, and (ii) δ_0 also is a homogeneous, isotropic Gaussian field and the power spectra of Φ_0 and δ_0 are uniquely related.

The description of the particle trajectories by equation (2.3) allows one to calculate the density field at any later time, in the framework of this approximation. This makes the Zel'dovich approximation particularly convenient for numerical studies. As we shall show next, it also allows us to calculate the power spectrum of the density fluctuations at any later time a, on scales for which equation (2.3) provides a useful approximation. We define the power spectrum $P(k, a)$ of the density fluctuations by

$$\langle\tilde\delta(\boldsymbol{k}, a)\,\tilde\delta^*(\boldsymbol{k}', a)\rangle=(2\pi)^6P(k, a)\,\delta_{\rm d}(\boldsymbol{k}-\boldsymbol{k}'), \tag{2.5}$$

where the brackets denote an ensemble average of realizations of the random field, $\delta_{\rm d}(\boldsymbol{k})$ is Dirac's delta 'function', and $\tilde\delta(\boldsymbol{k})$ is the Fourier transform of the density fluctuations,

$$\delta(\boldsymbol{x}, a)=\int \frac{\mathrm{d}^3k}{(2\pi)^3}\,\tilde{\delta}(\boldsymbol{k}, a)\mathrm{e}^{\mathrm{i}\boldsymbol{k}\cdot\boldsymbol{x}}. \tag{2.6}$$

The power spectrum $P(k, a)$ is the Fourier transform of the two-point correlation function $\xi(x, a)$ of the density field, which is defined as

$$1+\xi(x, a)=\frac{\langle\rho(\boldsymbol{x}', a)\rho(\boldsymbol{x}'+\boldsymbol{x}, a)\rangle}{\langle\rho\rangle^2(a)}, \tag{2.7}$$

or

$$\xi(x, a)=\langle\delta(\boldsymbol{x}', a)\,\delta(\boldsymbol{x}'+\boldsymbol{x}, a)\rangle,$$

where $\boldsymbol{x}$ is a vector of length x, and the angular brackets can be considered as denoting either an ensemble average, or an average over the vector $\boldsymbol{x}'$, which are equivalent assuming the ergodic hypothesis. One finds

$$P(k, a)=\int \frac{\mathrm{d}^3x}{(2\pi)^3}\,\xi(x, a)\mathrm{e}^{-\mathrm{i}\boldsymbol{k}\cdot\boldsymbol{x}}. \tag{2.8}$$

The two-point correlation function, more precisely $1+\xi(x, a)$, also may be derived from the probability of finding two particles (or 'fluid' elements) a distance x apart. Writing equation (2.3) in the form

$$\boldsymbol{x}=\boldsymbol{q}+\boldsymbol{s}, \tag{2.9}$$

where $\boldsymbol{s}=b\nabla\Phi_0(\boldsymbol{q})\approx a\nabla\Phi_0(\boldsymbol{q})$, and following MHP, we can write

$$1+\xi(x, a)=\int \mathrm{d}^3q\int \mathrm{d}^3s\,p(\boldsymbol{s}; \boldsymbol{q}, a)\,\delta_{\mathrm{d}}(\boldsymbol{x}-\boldsymbol{q}-\boldsymbol{s}), \tag{2.10}$$

where $p(\boldsymbol{s}; \boldsymbol{q}, a)\mathrm{d}^3s$ is the probability that two particles with initial separation vector $\boldsymbol{q}$ at a_{i} have undergone a relative displacement within d^3s of $\boldsymbol{s}$. In equation (2.10) we have assumed that the density fluctuations at $a=a_{\mathrm{i}}$ are very much smaller than unity, $\delta_{\mathrm{i}}(\boldsymbol{x})\ll 1$, so that all density inhomogeneities at later times $a\gg a_{\mathrm{i}}$ are caused predominantly by the displacement of the particles. As will be shown in Appendix A (see also MHP), the probability distribution $p(\boldsymbol{s}; \boldsymbol{q}, a)$ is

$$p(\boldsymbol{s}; \boldsymbol{q}, a)=\frac{1}{8\pi^{3/2}(U-V)\sqrt{(U-W)}}\times\exp\left[-\frac{s^2}{4(U-V)}-\frac{s_\parallel^2(W-V)}{4(U-V)(U-W)}\right], \tag{2.11}$$

with

$$U=a^2u=a^2\frac{4\pi}{3}\int_0^\infty \mathrm{d}k\,P_0(k),$$

$$V(q)=a^2v(q)=a^2 4\pi\int_0^\infty \mathrm{d}k\,P_0(k)\frac{j_1(kq)}{kq}, \tag{2.12}$$

$$W(q)=a^2w(q)=a^2 4\pi\int_0^\infty \mathrm{d}k\,P_0(k)\left(j_0(kq)-\frac{2j_1(kq)}{kq}\right);$$

$j_n(t)$ are the spherical Bessel functions, $s^2\equiv|\boldsymbol{s}|^2$, and $s_\parallel=\boldsymbol{s}\cdot\boldsymbol{q}/|\boldsymbol{q}|$. Note that, for large separations q, the functions V and W decrease like q^{-2}, i.e. the displacements of widely separated points are not correlated, since U is independent of q. Also, $v(0)=w(0)=u$. If we artificially set $V=0=W$, then $p(\boldsymbol{s}; \boldsymbol{q}, a)$ depends no longer on q, but only on s^2. v and w are even functions of q, which both behave like q^{-2} for $q\to\infty$. For example, if we use an HDM-like spectrum of the form $P_0(k)=Ak\mathrm{e}^{-\lambda k}$, we obtain

$$u=\frac{4\pi A}{3\lambda^2},$$

$$v(q)=\frac{4\pi A}{q^2}\left[1-\frac{\lambda}{q}\arctan\left(\frac{q}{\lambda}\right)\right],$$

$$w(q)=\frac{4\pi A}{\lambda^2+q^2}-2v(q).$$

Inserting (2.11) into (2.10), we obtain for the correlation function

$$1+\xi(x, a)=\int \mathrm{d}^3q\,p(\boldsymbol{x}-\boldsymbol{q}; \boldsymbol{q}, a)$$

$$=\int\frac{\mathrm{d}qq^2}{4\sqrt{\pi}(U-V)\sqrt{U-W}}\times\int_{-1}^{1}\mathrm{d}\mu\exp\left[-\frac{x^2(1-\mu^2)}{4(U-V)}-\frac{(x\mu-q)^2}{4(U-W)}\right], \tag{2.13}$$

in agreement with MHP (note that MHP have written the μ-integral in terms of Dawson's integral; however, since the sign of $(V-W)$ depends on the spectrum and on q, this may lead to an imaginary argument for Dawson's integral, which renders it less useful for practical calculations). As a check, we note that if we artificially set $V=0=W$ in equation (2.13), so that the displacements of the particles are no longer correlated, we get $\xi(x)=0$, as expected. If we rewrite (2.8) in the form

$$P(k, a)+\delta_{\mathrm{d}}(\boldsymbol{k})=\int\frac{\mathrm{d}^3x}{(2\pi)^3}[1+\xi(x, a)]\,\mathrm{e}^{-\mathrm{i}\boldsymbol{k}\cdot\boldsymbol{x}}$$

and insert (2.10) into this equation, the $\boldsymbol{x}$-integral can be done trivially, and we obtain

$$P(k, a)+\delta_{\mathrm{d}}(\boldsymbol{k})=\int \mathrm{d}^3q\,\mathrm{e}^{-\mathrm{i}\boldsymbol{k}\cdot\boldsymbol{q}}\int \mathrm{d}^3s\,p(\boldsymbol{s}; \boldsymbol{q}, a)\,\mathrm{e}^{-\mathrm{i}\boldsymbol{k}\cdot\boldsymbol{s}}. \tag{2.14}$$

Due to the Gaussian form of the probability distribution (2.11), the s-integration can be performed by choosing $\boldsymbol{k}$ to be aligned in k_3-direction, and for every $\boldsymbol{q}$ one can choose the s_1-axis such that $\boldsymbol{q}$ lies in the s_1–s_3-plane. The resulting exponent of the exponential can then be expanded in Cartesian coordinates s_i and integrated easily. The remaining q-integration is performed in spherical coordinates. The azimuthal-angle integration simply yields 2π, and after some algebra we end up with

$$P(k,a)=\frac{1}{2\pi^2}\int_0^\infty \mathrm{d}q\, q^2\left\{\exp[-a^2k^2(u-w)]\right.$$
$$\left.\times\int_0^1 \mathrm{d}\mu\cos(kq\mu)\exp[-a^2k^2(w-v)(1-\mu^2)]-j_0(kq)\right\}, \tag{2.15}$$

where the last term accounts for the contribution from the delta function; in fact, $\int \mathrm{d}q\, q^2 j_0(kq)$ vanishes for $k\neq 0$. As we shall see below, this term is cancelled by the leading-order term from the integral. Note that the quantities u, $v(q)$, $w(q)$ have been defined in equation (2.12). In order to make further progress, we observe that

$$\int_0^1 \mathrm{d}\mu\cos(A\mu)\exp[-B(1-\mu^2)]=\sum_{n=0}^{\infty}\left(\frac{-2B}{A}\right)^n j_n(A),$$

as can be seen by expanding the exponential and integrating term by term. Using the above relation in (2.15), we see that the leading-order term ($\propto a^0$) just cancels the last term in (2.15). We then obtain

$$P(k,a)=\frac{\exp(-a^2k^2u)}{2\pi^2}\int_0^\infty \mathrm{d}q\, q^2\left\{[\exp(a^2k^2w)-1]j_0(kq)\right.$$
$$\left.+\exp(a^2k^2w)\sum_{n=1}^{\infty}[2a^2k^2(v-w)]^n\frac{j_n(kq)}{(kq)^n}\right\}. \tag{2.16}$$

Since the Zel'dovich approximation was constructed to yield the same density distribution as the linear approximation for $\delta\ll 1$, which predicts $P(k,a)=a^2P_0(k)$, we expect that this linear result is contained in equation (2.16). The lowest order term of (2.16) is $\propto a^2$. By expanding the exponentials and inserting the definitions of v and w from (2.12) into (2.16), we obtain

$$\lim_{a\to 0}\frac{P(k,a)}{a^2}=\frac{2k^2}{\pi}\int_0^\infty \mathrm{d}t\,P_0(t)\int_0^\infty \mathrm{d}q\, q^2$$
$$\times\left\{\left[j_0(tq)-\frac{2j_1(tq)}{tq}\right]j_0(kq)\right.$$
$$\left.+\left[\frac{6j_1(tq)}{tq}-2j_0(tq)\right]\frac{j_1(kq)}{kq}\right\}.$$

The q-integrals over the products of spherical Bessel functions can be performed by writing the spherical Bessel functions in terms of ordinary Bessel functions and using equations (6.512.3) and (6.576.2) of Gradshteyn & Ryzhik (1980; hereafter GR); one then finds that the sum of the terms j_1j_0 and j_1j_1 just vanishes. The product j_0j_0 is integrated by multiplying the integrand by a factor $\exp(-\epsilon q^2)$, using GR(6.633.2), and then letting $\epsilon\to 0$. This results in a delta function; more specifically, the q-integration yields $\pi/(2k^2)\,\delta_{\mathrm{d}}(k-t)$, so that

$$\lim_{a\to 0}\frac{P(k,a)}{a^2}=P_0(k), \tag{2.17}$$

in agreement with the result from linear perturbation theory.

It should be noted that the transition from linear to non-linear behaviour depends not only on the scale factor a, but also on the magnitude of the wave vector for k; for very large k, the linear approximation breaks down already for small a. In fact, for $k\to\infty$, the power spectrum in the Zel'dovich approximation behaves like k^{-3}. This can be seen from equation (2.15), by noting that (i) for $k\to\infty$, only small values of q contribute significantly to the integral, (ii) the behaviour of $(u-w)$ and $(w-v)$ for small q is like bq^2, where b is a constant (see the remarks below equation 2.12), so that (iii) the bracket in equation (2.15) depends only on the combination kq, which yields the asymptotic behaviour immediately.

The asymptotic k^{-3}-behaviour has a simple physical origin. The pancakes which result from the prescription (2.3) of the particle trajectories are generic singularities of the Lagrangian mapping from $\boldsymbol{q}$-space to Eulerian $\boldsymbol{x}$-space. The density at such a caustic shows a universal behaviour, $\rho\propto\mathscr{L}^{-1/2}\mathrm{H}(\mathscr{L})$, where $\mathscr{L}$ is the distance of a point from the caustic (pancake). Thus the density distribution near a pancake is predominantly one-dimensional. If we consider a one-dimensional density profile of the form $\rho\propto\mathscr{L}^{-1/2}\mathrm{H}(\mathscr{L})$ in an interval, assuming periodic boundary conditions, it is easy to show that the one-dimensional power spectrum behaves like $P_1(k)\propto k^{-1}$. Then, by identifying $P_1(k)\,\mathrm{d}k=4\pi k^2P(k)\,\mathrm{d}k$, the universal $P_1(k)\propto k^{-3}$ immediately follows. This argument also shows that the k^{-3} asymptotic behaviour is not an artefact of the Zel'dovich approximation, but applies to all descriptions of the large-scale structure in which caustics form, provided that fold caustics are the most abundant and that dissipative processes are neglected even on small scales.

3 TRUNCATED ZEL'DOVICH APPROXIMATION AND THE POWER SPECTRUM

It is well known that the Zel'dovich approximation (2.3) yields a very useful description of the evolution of the density field well into the non-linear regime, until the formation of caustics begins. After these caustics (pancakes) have formed, the Zel'dovich approximation becomes less useful, since the compact structures become erased instead of being bound by self-gravity. A cure for this problem has been invented by letting the pancakes stick together once they have formed ('sticky dust' approximation: see Gurbatov, Saichev & Shandarin 1989; Shandarin & Zel'dovich 1989). The resulting 'adhesion approximation' (Weinberg & Gunn 1990) yields a surprisingly accurate description of the large-scale structure, when compared to N-body simulations which, however, also probe only a small range of non-linear scales.

Recently, a different method has been proposed to cure the Zel'dovich approximation of its largest deficit: Coles et al. (1993) introduced the 'truncated Zel'dovich approximation', in which the small-scale power is filtered away from the original power spectrum, in such a way as to prevent shell crossing and subsequent dissolution of pancakes from occurring too early. If the filter scale is chosen such that at the time of interest the smallest structures have just become non-linear, the results from the truncated Zel'dovich approximation compare very favourably with N-body results, even better than the adhesion approximation with respect to the comparison done by Melott (1994).

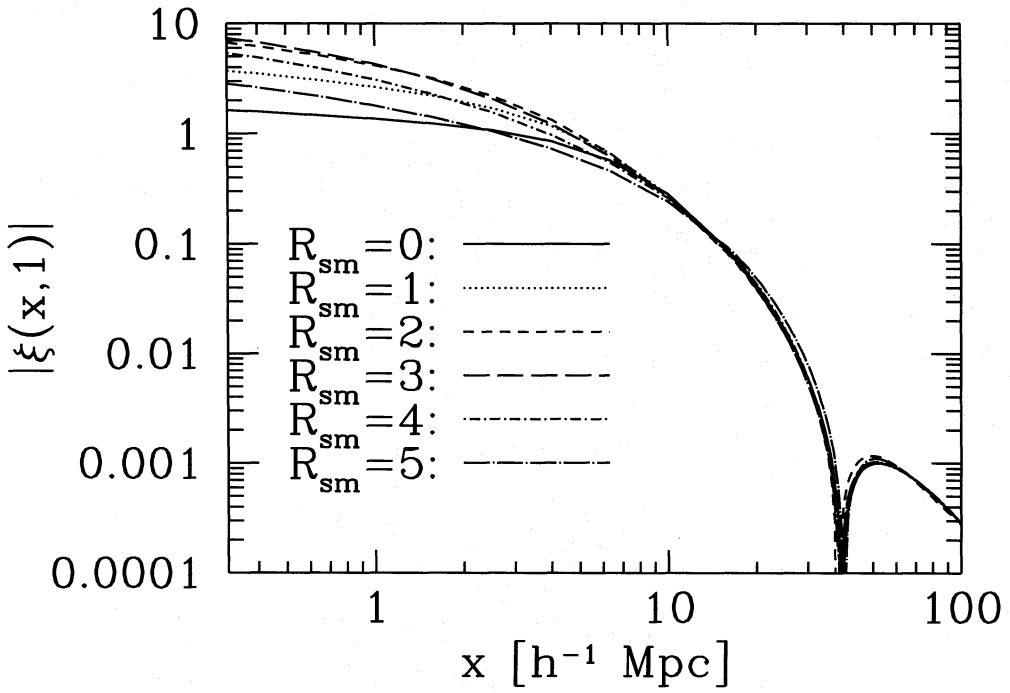

Figure 1. The two-point correlation function $\xi(x, 1)$ at the present epoch, for a truncated CDM spectrum with several smoothing scales (in h^{-1} Mpc) as indicated. It is clearly seen that $\xi(x, 1)$ attains a maximum for low x as a function of R_{sm}. For $x \gtrsim 10\ h^{-1}$ Mpc, the truncation has a negligible influence on the correlation function, which becomes negative for the first time at $x \approx 40\ h^{-1}$ Mpc.

In our notation, the truncated[1] Zel'dovich approximation is described by replacing the linearly extrapolated power spectrum $P_0(k)$ by

$$P_0(k, R_{sm}) \equiv P_0(k) \exp(-k^2 R_{sm}^2), \tag{3.1}$$

where the smoothing scale R_{sm} depends on the epoch at which one considers the evolved spectrum, which in the following will be denoted by $P_{tr}(k, a)$, and which is obtained by equation (2.15) if the truncated spectrum (3.1) is used in the calculation (2.12) of the coefficients u, v and w. Our choice of the filter scale $R_{sm}(a)$ agrees with that of MHP (and differs slightly from that of Melott 1994), in that we determine the two-point correlation function $\xi(x, a)$ for different values of R_{sm} and take that value of R_{sm} for which the correlation function becomes maximal for small x. In that way, the filter scale is chosen such that shell crossing is suppressed to a large degree. In Fig. 1, we have plotted the two-point correlation function $\xi(x, 1)$ for different values of the filter scale R_{sm}, using an unbiased CDM spectrum (Bardeen et al. 1986) as $P_0(k)$. This figure is very similar to fig. 1 of MHP and illustrates that there is a filter radius R_{sm} for which the correlation becomes maximal at small separations. $\xi(x, a)$ at $x = 1\ h^{-1}$ Mpc as a function of R_{sm} has a fairly broad maximum, so the best value of R_{sm} cannot be determined very accurately. We calculated that, within this accuracy, the optimal filter scale as a function of a for a CDM spectrum can be approximated by

$$R_{sm}(a) = 3.42(a - 0.2) H(a - 0.2)\, h^{-1}\ \text{Mpc}, \tag{3.2}$$

where $H(x)$ is the Heaviside step function; i.e. no smoothing is required for $a \lesssim 0.2$. In particular, $R_{sm}(1) = 2.74\ h^{-1}$ Mpc, in very good agreement with fig. 1 of MHP and numerical simulations of the truncated Zel'dovich approximation using the truncation scheme of Melott (1994; Buchert, private communication). For an HDM spectrum, no smoothing is required even at redshift $z = 0$ ($a = 1$).

We have calculated the power spectrum for a CDM and an HDM initial spectrum (normalized to the *COBE* quadrupole measurement of the microwave background fluctuations), with and without truncation in the former case, by integrating (2.16); some details of the calculations are provided in Appendix B. The results are displayed in Figs 2, 3 and 4.

Fig. 2 shows the power spectrum $P(k, a)/a^2$ for the HDM model and the power spectrum $P_{tr}(k, a)/a^2$ for the truncated CDM model. In the former case, a tail in the high-k regime develops, which is absent in the linear theory. It indicates the formation of structure on small scales, as described by the formation of pancakes. In the case of the truncated CDM spectrum, the power at large k is reduced relative to the linear theory, which illustrates that significant shell crossings occur despite the smoothing introduced above. Nevertheless, smoothing has a significant influence on the resulting spectrum, as shown in Fig. 3, where we compare the power spectra predicted by the Zel'dovich approximation for the truncated and untruncated cases. This figure shows that truncation increases the power on small scales by a large factor for small redshifts.

Finally, an alternative way to display our results is by noting that the power spectrum can be written as

$$P(k, a) = AkT^2(k, a), \tag{3.3}$$

where $T(k, a)$ is the transfer function and A is a normaliza-

[1]The scheme defined by equation (3.1) is Gaussian filtering rather than truncation, but we use the term 'truncation' in agreement with Melott (1994).

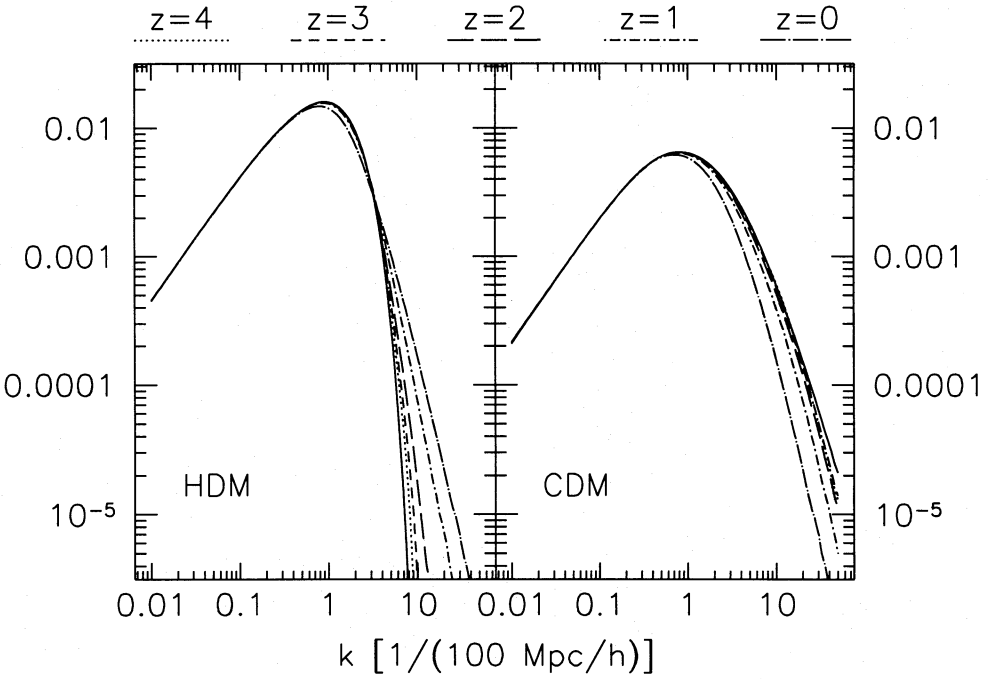

Figure 2. The power spectrum $P(k, a)/a^2$ in the (truncated) Zel'dovich approximation for unbiased CDM and HDM models. The solid curve in each case represents the spectrum $P_0(k)$ predicted from linear perturbation theory, whereas the other curves show the power spectra at $z = 0$, 1, 2, 3, 4, as indicated. For the CDM spectrum, the power spectrum has been truncated according to equations (3.1) and (3.2).

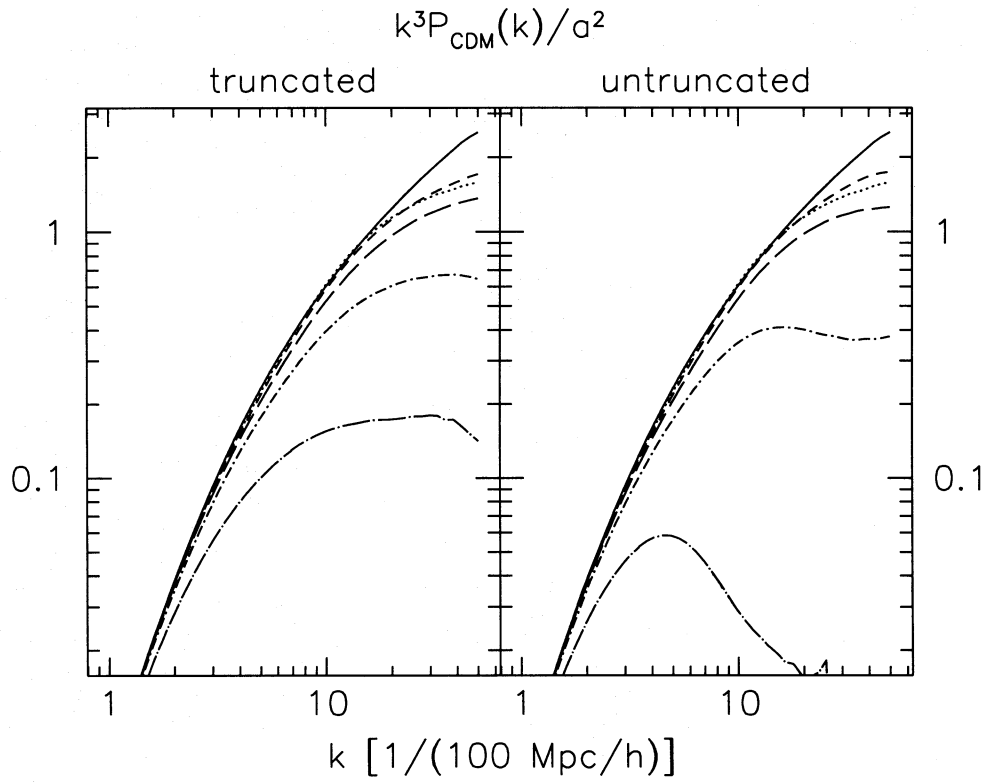

Figure 3. For a CDM model, the power spectrum in the truncated (left panel) and untruncated (right panel) Zel'dovich approximation is shown, here plotted as $k^3P(k, a)/a^2$, for redshifts $z = 0$, 1, 2, 3, 4 (line styles as in Fig. 2). A comparison between these two panels shows that the truncation predicts significantly more power on small scales for small redshifts than the untruncated power spectrum; in particular, $k^3P(k, a)$ is a monotonically increasing function in the former case.

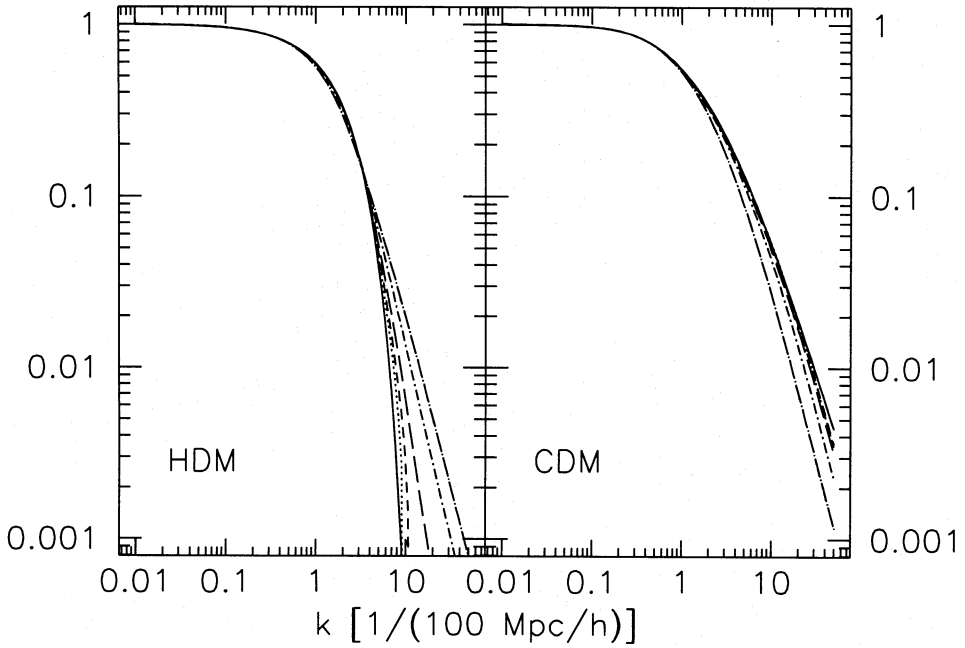

Figure 4. The effective transfer function $T(k, a)$ for the HDM and the truncated CDM model, as calculated in the Zel'dovich approximation. The solid curve represents the transfer function for $a \to 0$ and thus coincides with the usual definition of the transfer function. The other curves show the effective transfer function for redshifts $z = 0, 1, 2, 3, 4$, as indicated in Fig. 2.

tion constant. If we now consider (3.3) as a definition of $T(k, a)$ in terms of the power spectrum, we can calculate this effective transfer function for both models. This effective transfer function is displayed in Fig. 4.

Interestingly, the transfer function for HDM approaches a power law in k for $k \to \infty$ and $a \to 1$, which is very well approximated by

$$T_{\rm HDM}(k) \propto \frac{1}{k^2}. \tag{3.4}$$

This means that the spectrum attains a double-logarithmic slope of -3 for large k (as does the CDM spectrum) which has been predicted in Section 2. As mentioned there, this behaviour is a consequence of the universal properties of the density field close to fold singularities.

4 SUMMARY

We have calculated the power spectrum of density fluctuations in the Universe in the framework of the Zel'dovich approximation. The power spectrum can be expressed as a one-dimensional integral, the integrand of which depends on the initial power spectrum in a highly non-linear form, but reproduces the prediction from linear perturbation theory for small values of the cosmic scale factor a. The resulting spectra for a CDM and HDM model have been calculated; in the former case, the initial spectrum was truncated to suppress extensive shell crossings at early redshifts which erase true small-scale power. It has been found that small-scale power develops in the HDM model, in which the small scales are initially suppressed; in fact, for low redshifts the resulting spectra as predicted in the Zel'dovich approximation are about the same in both the (truncated) CDM and HDM models.

A comparison with numerically obtained power spectra in the (truncated) Zel'dovich approximation (Buchert & Weiss, private communication) shows excellent agreement with our results. Although the numerical determination of the power spectrum in the Zel'dovich approximation is fast and easy, it suffers from sampling problems and a finite dynamic range; neither of these problems hampers our determination.

ACKNOWLEDGMENTS

We thank T. Buchert, J. Ehlers and M. Hähnelt for detailed and constructive comments on the manuscript.

REFERENCES

Abramowitz M., Stegun I., 1984, Pocketbook of Mathematical Functions. Thun: Deutsch, Frankfurt/Main
Bardeen J. M., Bond J. R., Kaiser N., Szalay A. S., 1986, ApJ, 304, 15
Bond J. R., Couchman H. M. P., 1987, preprint
Buchert T., 1992, MNRAS, 254, 729
Buchert T., 1994, MNRAS, 267, 811
Buchert T., Ehlers J., 1993, MNRAS, 264, 375
Coles P., Melott A. L., Shandarin S. F., 1993, MNRAS, 260, 765
Gradshteyn I., Ryzhik I., 1980, Table of Integrals, Series, and Products. Academic Press, New York
Gurbatov S. N., Saichev A. I., Shandarin S. F., 1989, MNRAS, 236, 385
Mann R. G., Heavens A. F., Peacock J. A., 1993, MNRAS, 263, 798 (MHP)
Melott A. L., 1994, ApJ, 426, L19
Melott A. L., Buchert T., Weiss A. G., 1994, preprint MPA 799

Padmanabhan T., 1993, Structure Formation in the Universe. Cambridge Univ. Press, Cambridge
Press W. H., Teukolsky S. A., Betterling W. T., Flannery B. P., 1992, Numerical Recipes. 2nd edn, Cambridge Univ. Press, Cambridge
Shandarin S. F., Zel'dovich Y. B., 1989, Rev. Mod. Phys., 61, 185
Taylor A. N., 1993, in Bouchet F., Lachiéze-Rey M., eds, Proc. 9th IAP Conference, Cosmic Velocity Fields. Editions Frontière, Gif-sur-Yvette, p. 585
Weinberg D. H., Gunn J. E., 1990, MNRAS, 247, 260
Zel'dovich Y. B., 1970, A&A, 5, 84

APPENDIX A: DISPLACEMENT PROBABILITY DISTRIBUTION

In this appendix we derive the probability $p(\boldsymbol{s};\boldsymbol{q})\,\mathrm{d}^3s$ that two particles with initial comoving separation $\boldsymbol{q}$ have changed their separation by a value within d^3s of $\boldsymbol{s}$, where $\boldsymbol{s}$ has been defined below equation (2.9). Our derivation differs slightly from that of MHP and might be easier to follow.

Since $\boldsymbol{s}=a\nabla\Phi_0(\boldsymbol{q})$, we find from the Poisson equation (2.4) that the Fourier transform of $\boldsymbol{s}$ is

$$\tilde{\boldsymbol{s}}(\boldsymbol{k})=\mathrm{i}a\,\frac{\boldsymbol{k}}{|\boldsymbol{k}|^2}\,\tilde{\delta}_0(\boldsymbol{k}). \tag{A1}$$

Consider now two points $\boldsymbol{q}^{(1)}$ and $\boldsymbol{q}^{(2)}$ on the initial (Lagrangian) space, and denote their corresponding displacements by $\boldsymbol{s}^{(1)}$ and $\boldsymbol{s}^{(2)}$. Since $\boldsymbol{s}$ depends linearly on the density fluctuations δ, we find that, under the assumption that δ is a Gaussian random field, the joint probability distribution for the displacements $\boldsymbol{s}^{(m)}$, where $m=1,2$, must be a multivariate Gaussian distribution

$$p(\boldsymbol{s}^{(1)},\boldsymbol{s}^{(2)};\boldsymbol{q}^{(1)},\boldsymbol{q}^{(2)})=\frac{\exp(-\boldsymbol{S}\mathsf{A}^{-1}\boldsymbol{S}/2)}{(2\pi)^3\sqrt{\det\mathsf{A}}}, \tag{A2}$$

where $\boldsymbol{S}=(\boldsymbol{s}^{(1)},\ \boldsymbol{s}^{(2)})\in\mathbb{R}^6$ is a six-dimensional vector composed of the two separation vectors $\boldsymbol{s}^{(m)}$, and $\mathsf{A}\in\mathbb{R}^6\otimes\mathbb{R}^6$ is the covariance matrix with components

$$\mathsf{A}_{\mu\nu}=\langle S_\mu S_\nu\rangle \qquad 1\le\mu,\nu\le6. \tag{A3}$$

The components of A are calculated from (A3) and (A1) as

$$\begin{aligned}\langle s_i^{(m)}s_j^{(n)*}\rangle&=\int\frac{\mathrm{d}^3k}{(2\pi)^3}\exp(\mathrm{i}\boldsymbol{k}\cdot\boldsymbol{q}^{(m)})\\&\times\int\frac{\mathrm{d}^3k'}{(2\pi)^3}\exp(-\mathrm{i}\boldsymbol{k}'\cdot\boldsymbol{q}^{(n)})\\&\times a^2\,\frac{k_i}{|\boldsymbol{k}|^2}\,\frac{k'_j}{|\boldsymbol{k}'|^2}\,\langle\tilde{\delta}_0(\boldsymbol{k})\,\tilde{\delta}_0^*(\boldsymbol{k}')\rangle\\&=a^2\int\mathrm{d}^3k\,P_0(k)\,\frac{k_ik_j}{\langle\boldsymbol{k}\rangle^4}\exp[\mathrm{i}\boldsymbol{k}\cdot(\boldsymbol{q}^{(m)}-\boldsymbol{q}^{(n)})]\\&=\frac{4\pi}{3}a^2\int_0^\infty\mathrm{d}k\,P_0(k)\,m_{ij}[\boldsymbol{k}\cdot(\boldsymbol{q}^{(m)}-\boldsymbol{q}^{(n)})],\end{aligned} \tag{A4}$$

where in the last step we have defined

$$m_{ij}(t)=\frac{3}{4\pi}\int_0^{2\pi}\mathrm{d}\varphi\int_{-1}^{1}\mathrm{d}\mu\,\frac{k_ik_j}{|\boldsymbol{k}|^2}\,\mathrm{e}^{\mathrm{i}\nu\mu}, \tag{A5}$$

if we choose $\Delta\boldsymbol{q}=\boldsymbol{q}^{(2)}-\boldsymbol{q}^{(1)}$ to be parallel to the z-axis and μ is the cosine of the angle between $\boldsymbol{k}$ and $\Delta\boldsymbol{q}$. This yields

$$\begin{aligned}m_{11}(t)&=m_{22}(t)\equiv m_\perp(t)=3\,\frac{j_1(t)}{t},\\m_{33}(t)&\equiv m_\parallel(t)=3\left[j_0(t)-2\,\frac{j_1(t)}{t}\right],\\m_{ij}&=0\ \text{for}\ i\ne j.\end{aligned} \tag{A6}$$

This then leads to the matrix A:

$$\mathsf{A}=\begin{pmatrix}U&0&0&V&0&0\\0&U&0&0&V&0\\0&0&U&0&0&W\\V&0&0&U&0&0\\0&V&0&0&U&0\\0&0&W&0&0&U\end{pmatrix} \tag{A7}$$

where U, V and W have been defined in equation (2.12). The matrix A can easily be inverted:

$$\mathsf{A}^{-1}=\begin{pmatrix}X_1&0&0&Y_1&0&0\\0&X_1&0&0&Y_1&0\\0&0&X_2&0&0&Y_2\\Y_1&0&0&X_1&0&0\\0&Y_1&0&0&X_1&0\\0&0&Y_2&0&0&X_2\end{pmatrix} \tag{A8}$$

with $X_1=U/(U^2-V^2)$, $X_2=U/(U^2-W^2)$, $Y_1=-V/(U^2-V^2)$ and $Y_2=-W/(U^2-W^2)$. Together with $\det\mathsf{A}=(U^2-W^2)(U^2-V^2)^2$, the distribution function in (A2) is determined. The probability distribution for the relative displacement can then be obtained from

$$\begin{aligned}p(\boldsymbol{s};\Delta\boldsymbol{q})&=\int\mathrm{d}^3s^{(1)}\int\mathrm{d}^3s^{(2)}\,\delta_\mathrm{d}(\boldsymbol{s}-\boldsymbol{s}^{(2)}+\boldsymbol{s}^{(1)})\,p(\boldsymbol{s}^{(1)},\boldsymbol{s}^{(2)};\Delta\boldsymbol{q})\\&=\int\mathrm{d}^3s^{(1)}\,p(\boldsymbol{s}^{(1)},\boldsymbol{s}+\boldsymbol{s}^{(1)};\Delta\boldsymbol{q}).\end{aligned} \tag{A9}$$

The remaining integration can be factorized into three Gaussian integrals, which can be readily solved; the final result is given by equation (2.11). As expected, it depends only on the separation $|\Delta\boldsymbol{q}|$ and the components of $\boldsymbol{s}$ parallel and perpendicular to $\Delta\boldsymbol{q}$.

APPENDIX B: NUMERICAL DETERMINATION OF THE POWER SPECTRUM

The power spectrum as given in equation (2.16) has to be evaluated numerically. To do so, we first have to determine

the constant u and the functions $v(q)$ and $w(q)$, defined in equation (2.12). The determination of u is straightforward. Although the integrand in $v(q)$ oscillates due to the spherical Bessel function $j_0(kq)$, the envelope of the integrand decays rapidly enough to ensure that standard integration routines will succeed. This is not the case for the integrand of $w(q)$, however, where we need to apply methods designed for integrating functions modulated by oscillations $\propto \sin \omega x$. To do so, we first observe that $w(q)$ can be written

$$w(q) = w'(q) - 2v(q), \tag{B1a}$$

where

$$w'(q) = 4\pi \int_0^\infty \mathrm{d}k\, P_0(k) j_0(kq) = \frac{4\pi}{q} \int_0^\infty \mathrm{d}k \frac{P_0(k)}{k} \sin kq. \tag{B1b}$$

To evaluate $w'(q)$, we apply the routine DFTINT supplied by Press et al. (1992).

For large q, the integrands of $v(q)$ and $w'(q)$ are dominated by small k. There, the spectrum $P_0(k) \propto k$, and it follows that $v(q)$ and $w'(q)$ are both $\propto q^{-2}$. Moreover, we see from the definitions of u, $v(q)$ and $w'(q)$, and from the behaviour of $j_{0,1}(x)$ for $x \to 0$, that $v(q) \to u$ and $w'(q) \to 3u$ for $q \to 0$. The functions $v(q)$ and $w'(q)$ therefore naturally lend themselves to rational-function approximations, resulting in excellent fits of $v(q)$ and $w'(q)$ with only few coefficients (< 10), which are used further on in order to save computing time.

Having found u, $v(q)$ and $w(q)$, we can continue solving equation (2.16). Again we encounter the problem of integrating rapidly oscillating functions, which cause standard integration schemes to fail. To proceed, we first observe that each term in the infinite sum of equation (2.16) can be written in the form

$$I_n(k) = C \int_0^\infty \mathrm{d}q\, q^{2-n} f(q) j_n(kq), \tag{B2}$$

where C is a constant. These integrals are split according to

$$I_n(k) = C \sum_{i=1}^{\infty} \int_{a_i}^{a_{i+1}} \mathrm{d}q\, q^{2-n} f(q) j_n(kq) \equiv C \sum_{i=1}^{\infty} J_{in}(k), \tag{B3}$$

where $a_1 = 0$ and $a_\infty \to \infty$. Within each interval $D_i \equiv [a_i, a_{i+1}]$, the function $f(q)$ can be linearly interpolated; this assumption is well fulfilled if, for all i, the intervals D_i are sufficiently narrow.[2] We can therefore write

$$f(q)|_{D_i} = c_i q + d_i, \tag{B4}$$

where

$$c_i \equiv \frac{f(a_{i+1}) - f(a_i)}{a_{i+1} - a_i}, \tag{B5}$$

$$d_i \equiv f(a_i) - c_i a_i.$$

[2]This method can of course be straightforwardly generalized to local interpolation by a higher-order polynomial, in a similar manner to that used for the integration of trigonometrically oscillating functions in the routine DFTCOR of Press et al. (1992).

With $f(q)$ being linearly interpolated, the integrals $J_{in}(k)$ can be solved analytically. We define

$$J_{in}(k) \equiv c_i K_{in}(k) + d_i L_{in}(k) \tag{B6}$$

and obtain

$$K_{in}(k) \equiv \int_{a_i}^{a_{i+1}} \mathrm{d}q\, q^{3-n} j_n(kq),$$

$$L_{in}(k) \equiv \int_{a_i}^{a_{i+1}} \mathrm{d}q\, q^{2-n} j_n(kq). \tag{B7}$$

Using the recursion relation among spherical Bessel functions (e.g., Abramowitz & Stegun 1984, equation 10.1.19), we find

$$K_{in}(k) = \left[\frac{q^{4-n}}{3-2n} j_n(kq)\right]\Bigg|_{a_i}^{a_{i+1}} - \frac{k}{3-2n} K_{i,n-1}(k),$$

$$L_{in}(k) = \left[\frac{q^{3-n}}{2-2n} j_n(kq)\right]\Bigg|_{a_i}^{a_{i+1}} - \frac{k}{2-2n} L_{i,n-1}(k). \tag{B8}$$

It is evident from equation (B8) that these recursion relations can only be applied when $n > 1$; therefore we have to evaluate $K_{i0,1}(k)$ and $L_{i0,1}(k)$ explicitly. We obtain

$$K_{i0}(k) = \frac{2}{k^3}(a_{i+1} \sin ka_{i+1} - a_i \sin ka_i) - \frac{1}{k^2}(a_{i+1}^2 \cos ka_{i+1} - a_i^2 \cos ka_i) + \frac{2}{k^4}(\cos ka_{i+1} - \cos ka_i),$$

$$K_{i1}(k) = \frac{2}{k^3}(\cos ka_{i+1} - \cos ka_i) - \frac{1}{k^2}(a_{i+1} \sin ka_{i+1} - a_i \sin ka_i), \tag{B9}$$

$$L_{i0}(k) = \frac{1}{k^3}(\sin ka_{i+1} - \sin ka_i) - \frac{1}{k^2}(a_{i+1} \cos ka_{i+1} - a_i \cos ka_i),$$

$$L_{i1}(k) = \frac{1}{k^2}[\mathrm{Si}(ka_{i+1}) - \mathrm{Si}(ka_i)] - \frac{1}{k^2}(\sin ka_{i+1} - \sin ka_i),$$

where $\mathrm{Si}(x)$ is the sine integral. For any $n > 1$, the recursion relations (B8) can be applied. The sum (B3) is then evaluated for $1 \le i \le N$, where N has to be chosen such that the terms $J_{in}(k)$ for $i > N$ contribute negligibly to the result.

It turns out that, for $k \lesssim 0.5\ h\ \mathrm{Mpc}^{-1}$ it suffices to include terms with $0 \le n \le 3$ only; all terms with larger n are negligibly small.